Hamburger Beiträge
zur Angewandten Mathematik

Analysis of quasi-POMs in a microscopic traffic model

Bodo Werner

Nr. 2011-15
August 2011

Analysis of quasi-POMs in a microscopic traffic model

Bodo Werner

August 3, 2011

Abstract

This paper is an extension of [GW10, SGW09] where a microscopic follow-the-leader-model of N identical cars on a circle S^1_L of length L, with bottleneck like road works, were studied. It was shown that Ponies-on-a-Merry-Go-Round-solution's (POM's) can bifurcate to so called quasi-POMs, where the length L and the strength ε of the bottleneck are chosen as bifurcation parameters.

In this paper our focus is on quasi-POMs, particularly their macroscopic visualizations, where the trajectories $(\xi_j(t), t)$, $\xi_j(t) := x_j(t) \bmod L$ are colored according to the speed $v_j(t) = \dot{x}_j(t), j = 1, 2, .., N$. In the simulations in [GW10] we had observed a time periodicity of these macroscopic visualizations (see Fig. 1). This will be analyzed in this paper. As a consequence quasi-POMs are shown to have a macroscopic time-period T_p under a certain assumption**A**.

To perform our analysis we investigate the closed invariant curves γ of reduced Poincaré maps π. The notion *quasi-POM* is based on the appearance of an invariant curve of π. Restricting π to γ we obtain circle diffeomorphisms f such that we can apply the theory for circle maps as presented in [GH83] and [dMvS91]. We have to make an assumption which includes the irrationality of the rotation number ϱ of the circle map. We obtain a connection between the macroscopic period T_p, the rotation number ϱ of the circle map and the average wait time τ between two successive passings of cars at the observer point ξ_M of the circle associated with the reduced Poincaré map. Based on a numerical algorithm for the computation of T_p, very similar to the McKay algorithm computing ϱ, we are able to construct analytically and numerically a continuous macroscopic speed function $v(\xi, t)$, depending on the space variable $\xi \in S^1_L$ and on time t, periodic with time-period T_p, and interpolating the discrete data $v_j(t) = \dot{x}_j(t)$ in $(\xi_j(t), t)$ with $\xi_j(t) := x_j(t) \bmod L$.

The average wait time τ is connected with the global flow $f = 1/\tau$ of the quasi-POM. It will be compared with the global flows of coexisting POMs (where $v(\xi, t)$ is independent on time t).

Keywords: traffic flow, circle maps, rotation number, Hopf bifurcation, Neimark–Sacker bifurcation, quasi-periodic solution

AMS subject classification: 37M20, 65L07, 65P30, 65P40

1 Introduction

This paper can be considered as a theoretical attachment to [GW10], where a microscopic follow-the-leader-model on a circle S^1_L of length L with bottleneck like road works was studied. We again assume that there are N "identical" cars, obeying the same optimal velocity function. Our focus here is on quasi-POMs which bifurcate from Ponies-on-a-Merry-Go-Round-solution's (POMs). The bifurcation parameters are the strength ε of the bottleneck and the length L of the circle.

Quasi-POMs are special solutions of the ODE system which are identified by so-called invariant curves γ of reduced Poincaré maps π, while POMs correspond to their fixed points. Quasi-POMs may be the result of Neimark-Sacker type bifurcation for the map π. The reduced Poincaré map π involves an observer somewhere at a measure point $\xi_M \in S^1_L$. Every time when a car passes ξ_M, the configuration $\mathbf{x}$ of the whole car ensemble (positions and velocities of all cars) yields a point of a discrete orbit under π lying on γ.

In [GW10] we have seen that the macroscopic visualizations of quasi-POMs where the car trajectories in the (ξ, t)-plane are colored according the size of speed, show time-periodic traffic patterns. For an example from [GW10] see Fig. 1. The time-periodicity is obvious. The period can be roughly estimated by $T_p \approx 30$.

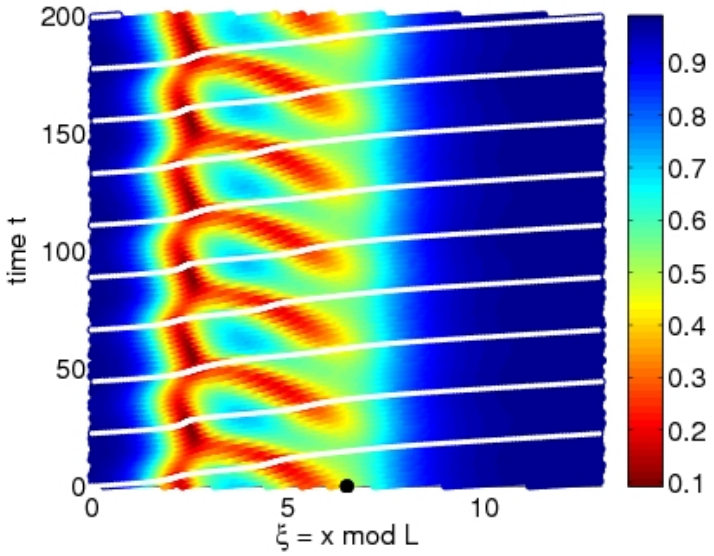

Figure 1: $N = 10, L = 13, \varepsilon = 0.3$: Macroscopic visualization of a quasi-POM from [GW10].

Under certain assumptions, we are going to prove this observed macroscopic time periodicity, by analyzing the invariant curves γ associated with the quasi-POMs using dynamical system theory of circle maps. Up to now, the invariant curves γ were only a tool to identify quasi-POMs.
To understand our analytical approach we have to look more carefully at the invariant curves γ. Fig. 2 shows the projection of γ on the speed-headway plane of a single car close to the center of the bottleneck. Here also the first ten orbit points under the reduced Poincaré map are numbered. The rather small distance of two successive points of the orbit indicates a rather small rotation number ϱ.
The invariant curve γ lives in $\mathbb{R}^{2N-1}$, where N is the number of cars. Every $\mathbf{x} \in \gamma$ is a possible observed configuration of the whole car ensemble by the observer at the measure point ξ_M which defines the reduced Poincaré map. Introducing suitable angle coordinates, the flow of our ODE system, restricted to γ, can be interpreted as an orientation preserving diffeomorphism f of the circle $S^1 := \mathbb{R}/\mathbb{Z}$. The classical theory of such circle maps is well known, see DE MELO, VAN STRIEN [dMvS91], GUCKENHEIMER-HOLMES [GH83]. The most prominent notion is that of a **rotation number** $\varrho \in [0, 1)$ which we assume to be irrational such that the map is ergodic and the Birkhoff Ergodic Theorem applies.
Under a certain assumption which we denote by **A** (see the end of this section), we prove

$$T_p = \frac{\tau}{\varrho} \tag{1}$$

for the time period T_p of the macroscopic pattern, where τ is the average wait time the observer has to wait between two successive passings of cars. τ has a simple traffic relevance, since the global flow f of the dynamics is given by

$$f = \frac{1}{\tau} = \frac{1}{\varrho \cdot T_p}. \tag{2}$$

Further, there is a numerical algorithm, due to MACKAY [Mac92], for the efficient computation of the rotation number. Remarkably. the rotation number ϱ can be included by convergents of the continuous fraction expansion of ϱ. It turns out that this algorithm can be extended to compute and even to include the period T_p by lower and upper bounds.
As another consequence, we can show that a quasi-POM is associated with a macroscopic continuous speed function $v(\xi, t)$ being T_p-periodic in the time variable t and interpolating the discrete speed datas $v(\xi_j(t), t) = \dot{x}_j(t), j =$

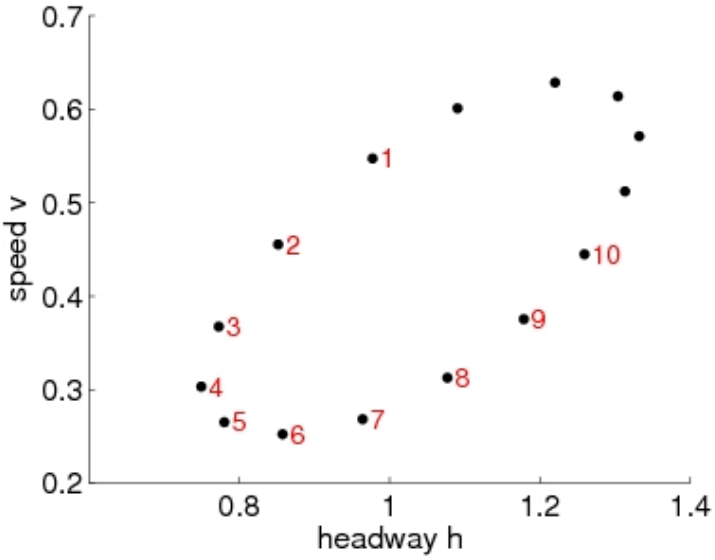

Figure 2: $N = 10, L = 13, \varepsilon = 0.3$ Invariant curve for car No. 4 (counted from the measure point $\xi_M = 0$). The rotation number is $\varrho = 0.068$.

$1, 2, ..., N$ (Theorem 1). The resolution in Fig. 1 is not appropriate to see the discreteness of our macroscopic visualization since time runs through a too large time interval. Fig. 3 is more appropriate for this purpose. Here the trajectories are shown only for $t \in [0, T_p]$ with $T_p = 32.7$ being computed by the MacKay Algorithm.
Once the period T_p is known, the macroscopic function $v(\xi, t)$ can be numerically approximated by a simple numerical simulation of the ODE system over a certain number m of time intervals of length T_p. Time runs from $t = 0$ to $t = m \cdot T_p$, for $0 \leq t \leq m \cdot T_p$ we set

$$v(\xi, s) = \dot{x}_j(t), \text{ whenever } \xi = x_j(t) \bmod L,\ s = t \bmod T_p \text{ for } j = 1, ..., N. \tag{3}$$

We call the method to compute $v(\xi, t)$ by (3) *projection method*. With respect to a satisfactory visualization we would like to get a set

$$\{(x_j(t) \bmod L, t \bmod T_p), j = 1, 2, ..., N, t \in [0, m \cdot T_p]\}$$

being visually dense in $[0, L] \times [0, T_p]$. The number m which is needed for this purpose, depends on properties of ϱ and on the chosen plot thickness of the visualized trajectories. The smaller ϱ and the more irrational ϱ is, the smaller m. For the example in Fig. 1-3 ($T_p = 32.7$) the continuous result in Fig. 4 has been obtained for $m = 10$, e.g. the simulation was performed from $t = 0$ until $t = 10 \cdot T_p = 327$.

At the end of the Introduction we want to sketch the idea behind our analysis. We use notations in the context of tori solutions (quasi-periodic) where a Poincaré map π and a smooth invariant curve γ of π with angle coordinates[1] $\varphi \in S^1 = [0, 1)$ and circle map f are involved. We assume that the rotation number $\varrho = \varrho(f)$ is irrational.
Before we are doing this, we want to discuss the link between the invariant curve γ associated with an observer at ξ_M and the macroscopic graphical representation of the quasi-POM. Assume that a car passes ξ_M at certain time t_M. The whole car configuration at time t_M is a point $\mathbf{x}(\varphi_M) \in \gamma$, represented by the N points $x_j(t_M) \bmod L$ on the trajectories colored according to $\dot{x}_j(t_M), j = 1, 2, ..., N$. The angle φ_M is somewhere hidden in the time t_M, it cannot been observed directly, unless γ is known and the specific polar coordinates for γ are fixed. A finite number of points of the invariant

[1] In the numerical part we have to assume that suitable polar angles as in Fig. 5 can be chosen.

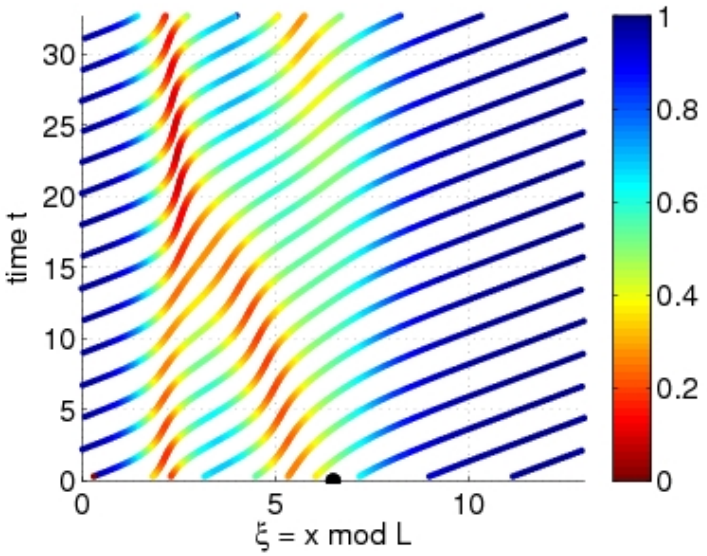

Figure 3: Discrete macroscopic visualization of a quasi-POM (MakroN10L13ep0,3SingleOrbits)

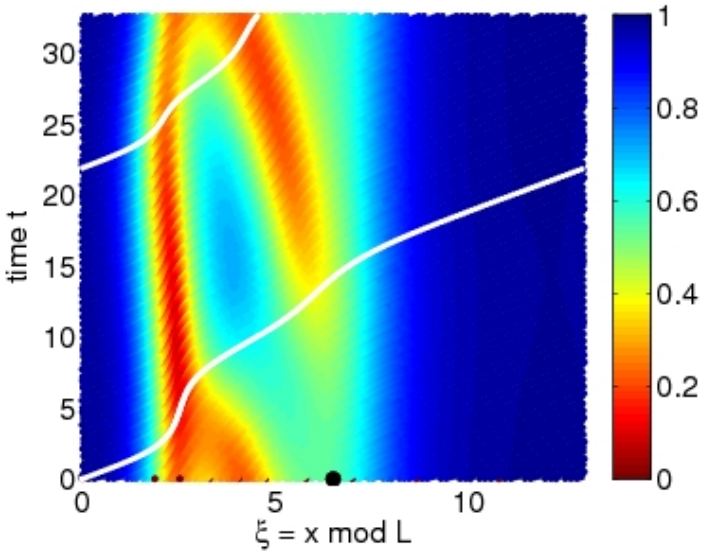

Figure 4: $N = 10, L = 13, \varepsilon = 0.3, T_p = 32.7$, quasi-POM: Macroscopic visualization of $v(\xi, t)$ by projection.

curve could be reconstructed by the macroscopic picture taking all discrete times t_n where a car is passing ξ_M and all positions $\xi_j(t_n) = x_j(t_n) \bmod L$ and speeds $\dot{x}_j(t_n), j = 1, 2, ..., N$.
Now assume that there is a scalar field v on γ which can be observed, for instance the speed or headway of a certain car. We will focus on that car which passes the observer point. This function v is measured at the discrete observer times t_n together with the discrete states $\mathbf{x}(\varphi_n) \in \gamma$, where φ_n is the corresponding angle on γ. The aim is to show that there is a time-period T_p and a T_p-periodic function $v(t)$ which interpolates the discrete observed data $v(t_n)$. The main tool is a connection between angle coordinates φ_n and the observer times t_n.

1. We introduce the *wait time* $\tau(\varphi)$ between the Poincaré event associated with φ and the next event. Using the Birkhoff Ergodic Theorem there is an *average wait time* τ and a *time T_p of circulation of* γ, with $T_p = \frac{\tau}{\varrho}$, where ϱ is the rotation number of f. The three numbers ϱ, τ and T_p do not depend on the special Poincaré section defining the Poincaré map (and the invariant curve γ), but only on the quasi-POM.

   The aim is to show that T_p can be interpreted as the macroscopic time period.

2. We consider a continuous scalar field v on γ (as for instance the speed of the car passing the observer). v can be extended to a real 1-periodic function $v = v(\varphi), \varphi \in S^1$.

3. Introduce the "modulo time" $s := t \bmod T_p$.

4. Our assumption **A**: There is an orientation preserving homeomorphism $\Phi : s \mapsto \Phi(s)$ between the circle $S^1_{T_p}$ of times and the circle S^1 of angles on γ. Φ is called the time-angle-function.

   Equivalent to assumption **A** is that the orbit (s_n) of modulo-times has the same ordering as the orbit (φ_n) under f. Or: The modulo times s/T_p is a suitable S^1-coordinate on γ where now the rotation angle is the average wait time divided by T_p.

5. Set $V(s) := v(\Phi(s))$. Then V can be extended to a continuous T_p-periodic real function $V(t)$.

6. Assume that there is a one-parameter family of Poincaré maps depending continuously on a parameter ξ (like $\xi = \xi_M$). Then we obtain a macroscopic scalar field $V(\xi, t)$ being T_p-periodic and continuous in t and continuously in ξ.

It would be interesting to discuss the transfer of our analysis to quasi-periodical solutions of more general ODEs.

2 The model

Following [SGW09, GW10] we shortly present the traffic model for the case where all cars obey the same driving law — all drivers are assumed to be "identical".
We study the situation of N cars on a circular road of length L. A widely used car following model describing such a situation is the optimal velocity model introduced by Bando et al. [BHN+95].
The optimal velocity function $V = V(d)$ expresses the velocity a car is aiming to achieve, according to the distance d (the headway) to the car in front. This function $V : [0, \infty) \to [0, \infty)$ is assumed to be smooth and strictly monotone increasing, satisfying $V(0) = 0$ and $\lim_{d\to\infty} V(d) = V_{max}$.
In [SGW09], a bottleneck (caused for example by roadworks) was introduced by extending the optimal velocity function to

$$V_\epsilon(\xi, y) = \left(1 - \epsilon e^{-(\xi - \frac{L}{2})^2}\right) V(y). \tag{4}$$

The bottleneck is centered around the position $\xi = \frac{L}{2}$ and it acts by reducing the maximal velocity. The parameter $\epsilon \geq 0$ describes the "strength" of the bottleneck. We are interested in the dynamics of the traffic in dependence on the parameter ε and the length L of the circle. The latter controls – for fixed N – the traffic density on the circle.

Let $x_j = x_j(t), t \geq 0$, be the distance the j-th car has covered at time t. We do not allow overtaking (as in [BJ08]) and hence assume $x_1 < x_2 < \cdots < x_N$. In the following we set $\xi_j = x_j \mod L, \quad j = 1, ..., L$, the positions of the cars on the circle.
The ODE model reads as

$$\left\{ \begin{array}{rcl} \dot{x}_j & = & v_j \\ \dot{v}_j & = & \frac{1}{\tau}(V_\varepsilon(\xi_j, x_{j+1} - x_j) - v_j) \end{array} \right\}, \quad j = 1, \ldots, N, \quad x_{N+1} = x_1 + L. \tag{5}$$

The circular road is represented by the fact that $x_{N+1} = x_1 + L$. We recall some results for this simplest version of identical drivers, first without bottleneck.

2.1 The case without bottleneck

Here, no explicit dependence on the position due to a bottleneck is given.

$$\left\{ \begin{array}{rcl} \dot{x}_j & = & v_j \\ \dot{v}_j & = & \frac{1}{\tau}(V(x_{j+1} - x_j) - v_j) \end{array} \right\}, \quad j = 1, \ldots, N, \quad x_{N+1} = x_1 + L. \tag{6}$$

This is the model presented originally by Bando et al [BHN+95]. It was studied by various authors (see [GSW04] and references therein), recently also by the author ([Wer11]).
Although the model is very simple it became an important tool in the description of traffic flow on a circular road. Many phenomena discovered in real experiments on a circular road setting can be described by the simple model (6). This is related to the fact, that there exist simple solutions – called *quasi-stationary solutions* – given by

$$x_j^0(t) = j \cdot \frac{L}{N} + t \cdot V\Big(\frac{L}{N}\Big), \qquad j = 1, ..., N. \tag{7}$$

The terminology quasi-stationary solution is due to the fact that this solution itself is (obviously) not stationary, but the corresponding velocities $v_j^0 = V(\frac{L}{N})$ and headways $d_j^0 = \frac{L}{N}$ are.
Stability criteria and formulas for critical parameter values where Hopf bifurcations occur, can be determined. The bifurcating periodic solutions which we will call *hopf-periodic* show well known oscillations in headway and and velocity. They can be interpreted as traveling waves.

2.2 The case with bottleneck

In the case of bottleneck we use the model (5). Here quasi-stationary solutions of type (7) do not exist any more. It came out that so called rotation solutions are the right object to look for (see [SGW09]).
A rotation solution of (5) with orbital period T is defined by

$$x_j(t + T) = x_j(t) + L, \quad v_j(t + T) = v_j(t), \quad j = 1, 2, ..., N, \tag{8}$$

where T is assumed to be minimal.
We see that for $\varepsilon = 0$, our quasi-stationary solutions are (trivial) rotation solutions with *orbital period* $T := L/c$, where $c = V(L/N)$ is the common velocity of the drivers. But observe that the Hopf-periodic solutions we get by Hopf bifurcations in general are *not* rotation solutions with orbital period T. Rotation solutions are nothing else then special periodical solutions when our ODE is considered on a manifold given by $(S^1_L \times \mathbb{R})^N$.
Since all drivers are assumed to be identical, one can add an additional symmetry condition to a rotation solution, namely

$$x_j(t + T/N) = x_{j+1}(t) \text{ for all } t, \quad j = 1, 2, ..., N. \tag{9}$$

This means that all cars behave in the same way except a time shift of T/N between two cars. Rotation solutions satisfying (9) are known as Ponies-on-a-Merry-Go-Round-solution's (POMs) (see [AGMP91, SGW09]).

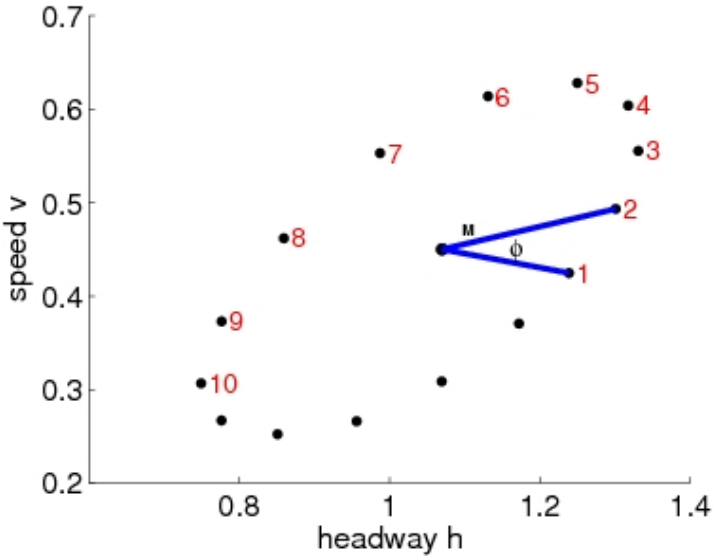

Figure 5: $N = 10, L = 13, \varepsilon = 0.3$ Invariant curve $\tilde{\gamma}$ for car No.4 with polar angle ϕ and center M.

It turns out that the method to investigate rotation solutions via Poincaré maps Π can be simplified considerably. The additional condition (9) allows to pass to a so called *reduced* Poincaré maps π, and the theoretical and numerical analysis of POMs can be based on π in a very efficient way. The return time for π is approximately the Nth fraction of that for Π. While the Poincaré map Π (see [SGW09]) looks for discrete times whenever the car number say with No. 1 passes a observer at position ξ_M, the reduced Poincaré map lists the whole configuration $\mathbf{x}$ (position and velocities) at discrete times whenever *any* car passes the position $\xi = 0$. This gives a denser discrete time grid on which dynamics is evaluated. The return time of π can be interpreted as a time the observer at the measure point ξ_M has to wait between two successive passings of cars. In the next section we use the notation *wait time*.
Now, POMs correspond to fixed points and *quasi-POMs* to invariant curves of π which may bifurcate in Neimark–Sacker points of π. This is the way how quasi-POMs are identified. Again, quasi-stationary solutions correspond to POMs and Hopf-periodic solutions to quasi-POMs.

3 Theory

In this section we are going to prove that, under mild conditions, quasi-POMs have a macroscopic time period T_p being observed in Fig. 1. As outlined in the Introduction, the invariant curves γ of the reduced Poincaré maps π and the circle maps f induced by the restriction of π to γ play an essential role in the analysis.

3.1 Theory of circle maps

We assume that γ is sufficiently smooth and that f is an orientation preserving circle diffeomorphism using suitable angle coordinates for γ. A natural choice can be a polar angle φ of the projection of γ onto a headway-speed-plane of some fixed car (call this projection $\tilde{\gamma}$) with respect to a "center" M, see Fig. 5 as an example, where the interior of $\tilde{\gamma}$ is star-shaped with respect to M.
It is convenient to identify the invariant curve γ with $S^1 = [0, 1)$, hence angles are varying from $\varphi = 0$ to $\varphi = 1$. Note that φ is the coordinate of γ in contrast to ξ, the coordinate of the traffic circle S^1_L of length L.

Our focus now is on the circle map f, given by the restriction of π to γ, and the theory of circle maps, as for instance presented in DE MELO, VAN STRIEN [dMvS91] and GUCKENHEIMER-HOLMES [GH83]. Most important is the **rotation number** $\varrho \in [0,1)$ of f, defined by the time average of the rotation angle along any orbit under f which is independent of the initial angle of the orbit.
In the following we assume that ϱ is irrational and that f is sufficiently smooth such that Denjoy's Theorem holds. This theorem claims that any orbit under f is dense on γ and that there are special angle coordinates on γ such that f is described by a simple rotation r_ϱ about the angle ϱ with respect to these coordinates. In other words: f is topologically conjugate to the rotation r_ϱ. Moreover, there is an invariant measure μ such that the Birkhoff Ergodic Theorem (see DE MELO, VAN STRIEN p.50 [dMvS91]), holds which claims that for all continuous real functions g on γ the time average

$$\lim_{n\to\infty} \frac{1}{n} \sum_{j=0}^{n-1} g(f^j(\varphi_0)) = \int_\gamma g d\mu \quad \text{for all } \varphi_0 \tag{10}$$

exists[2] and equals the space average of g.
Our invariant curve γ and the induced circle map f depend on the measure point $\xi_M \in S^1_L$ by which the Poincaré section is defined. But the circle maps associated with different measure points are diffeo-conjugate (the diffeomorphism is the flow from one hyperplane to the other), and hence have the same rotation number. Therefore, the rotation number ϱ is a characteristic number of the quasi-POM, not only of the invariant curve γ (which varies with the measure point).
Possible functions g in (10) are given by the speed or the headway of a single car or – for us most interesting – by the time an observer at the measure point (for instance at $\xi_M = 0$), observing $\mathbf{x} \in \gamma$ (and implicitly the corresponding angle[3] φ), has to wait until the next car will pass the measure point when $\pi(\mathbf{x})$ (respectively the corresponding angle $f(\varphi)$) is observed. This *wait time* turns out to be crucial for our analysis. Observe that any point $\mathbf{x} \in \gamma$ is a possibly observed configuration of the whole car ensemble, and $\pi(\mathbf{x})$ is the configuration when the next car shows up at the measure point.
Any orbit of f given by the angle sequence (φ_n), is associated with such wait times $\tau_n > 0, n = 1, 2, ...$ The time being passed when the nth observation is performed, is given by the sum $t_n := \tau_0 + \tau_1 + \cdots + \tau_{n-1}$. Of course, the wait time $\tau(\varphi)$ defines a smooth real function on γ, and by the Birkhoff Ergodic Theorem (10),

$$\tau := \lim_{n\to\infty} \frac{t_n}{n} \tag{11}$$

exists and can be interpreted as the average wait time at the given measure (observer) point. τ is independent of the special orbit, initiated by φ_0 and also independent of the observer point[4]. Hence the average wait time τ is, besides of ϱ, another invariant of the quasi-POM.
We keep in mind that the orbit (φ_n) is associated with a real time sequence (t_n) where t_n is the overall time being passed when φ_n is observed.
Now we are going to approach the (macroscopic) time period T_p. An obvious guess is that it equals the time an orbit under f needs to circle γ (*time of circulation*). We just counter the number $z_n \in \mathbb{N}_0$ of γ-rounds the orbit has finished at a certain time t_n. Then, the time of circulation is approximately given by t_n/z_n. Since

$$\varrho = \lim_{n\to\infty} \frac{z_n}{n},$$

we have

$$T_p := \lim_{n\to\infty} \frac{t_n}{z_n} = \lim_{n\to\infty} \frac{t_n}{n} \cdot \frac{n}{z_n} = \lim_{n\to\infty} \frac{t_n}{n} \cdot \lim_{n\to\infty} \frac{n}{z_n} = \frac{\tau}{\varrho}. \tag{12}$$

If we scale time by $t \mapsto s := t/T_p$ the average wait time is just the rotation number ϱ. Note that the time of circulation T_p is (together with ϱ and τ) another invariant of our quasi-POM.

The essential step is to link the time of circulation T_p in (12) to our macroscopic time period.

[2] The convergence is uniformly wrt to the initial angle φ_0.
[3] by a kind of a posteriori analysis after having found γ.
[4] For another measure point the times t'_n satisfy $|t_n - t'_n| \leq C$ for a constant C.

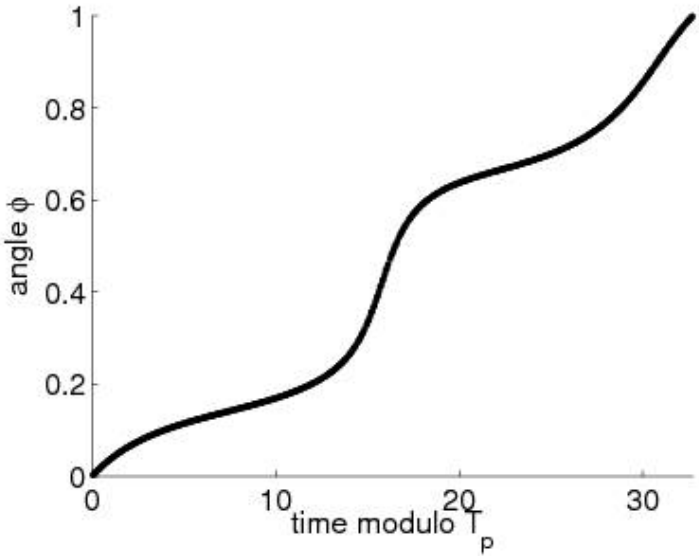

Figure 6: time-angle function Φ for the invariant curve in Fig. 5, $T_p = 32.74$

We consider a single orbit under f on γ, starting in φ_0 at time $t_0 = 0$. Any orbit point φ_n under f is associated with $\mathbf{x}_n \in \gamma$, an observation time t_n, a wait time $\tau_n := t_{n+1} - t_n$ and some scalar quantity v_n like the speed v_n of the car passing the measure point ξ_M (we assume now an arbitrary $\xi_M \in [0, L)$).
It is natural to introduce the "modulo-time" $s_n := t_n \bmod T_p$. Observe that $\mathbf{x}_n \in \mathbb{R}^{2N-1}$ contains all informations of the car ensemble at time t_n. If T_p is our desired macroscopic time-period of a continuous speed function $v : S^1_L \times [0, \infty) \to \mathbb{R}, (\xi, t) \mapsto v(\xi, t)$, the statement $v(\xi_M, s_n) = v_n$ must hold. If (s_n) is dense in $[0, T_p)$ and $v(\xi, .)$ is continuous, the sequence (v_n) would uniquely define our desired function $v(\xi_M, \cdot)$.
Observe that we encounter three types of circles. First the traffic circle S^1_L of length with variable ξ, second the γ-circle S^1 with variable φ and third the time-circle $S^1_{T_p}$ of length T_p.

As outlined in the Introduction, an essential step is the following assumption.

Assumption A: The orbit (s_n) in $[0, T_p) = S^1_{T_p}$ has the same ordering as $(\mathbf{x}_n)$ on γ, respectively as (φ_n) on $S^1 = [0, 1)$. This means that whenever we stop the orbit at a discrete time n, any point φ_j is the left (right) neighbor of φ_k on S^1 if and only if s_j is the left (right) neighbor of s_k.

Under this assumption **A**, with (φ_n) also (s_n) is dense in $[0, T_p]$, and it follows as in the proof of Denjoy's Theorem (GUCKENHEIMER-HOLMES [GH83]) that there is a coordinate transformation $\Phi : s \mapsto \varphi$, satisfying $\Phi(s_n) = \varphi_n, n = 1, 2, ...$ defining an orientation preserving homeomorphism. We call Φ the time-angle function. After having computed T_p, we may draw $s_n \mapsto \varphi_n, n = 1., 2, ..., n$, see Fig. 6.
Remark: The following three conditions are equivalent to assumption A.

1. The sequence (s_n) in $S^1_{T_p}$ has the same ordering as (φ_n) on S^1.
2. There is an orientation preserving homeomorphism[5] $\Phi : S^1_{T_p} \to S^1$ satisfying $\Phi(s_n) = \varphi_n, n = 0, 1, 2, ...$
3. (s_n/T_p) is a suitable angle coordinate on S^1 instead of φ.

[5]There exists a strictly monotone increasing lift $\hat{\Phi} : \mathbb{R} \to \mathbb{R}$ satisfying $\hat{\Phi}(t + k \cdot T_p) = \Phi(t) + k$ and $\hat{\Phi}(t) = \varphi(t)$ for $t \in [0, T_p)$.

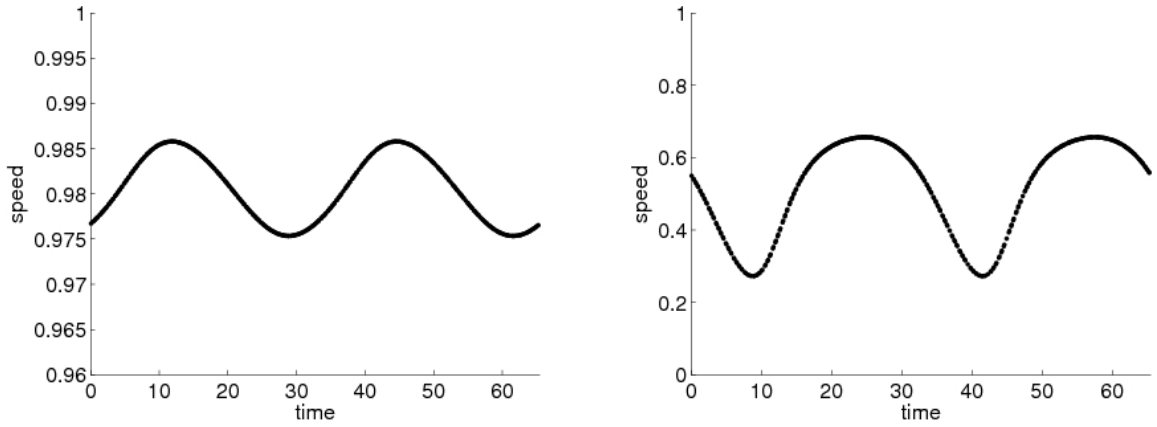

(a) $\xi = 0$ (b) $\xi = L/4$

Figure 7: $t \mapsto v(\xi, t)$ for the invariant curve in Fig. 5, $T_p = 32.74, n = 400$

Hence, assumption A can be numerically checked by drawing the time-angle function like in Fig. 6.

Theorem 1. *Let $T_p := \frac{\tau}{\varrho}$ be defined as in (12). Let the assumption* **A** *hold. Then for each continuous state v (like the speed of a single car) and for each observer point $\xi \in S^1_L$ there is a unique T_p-periodic continuous function $v(t)$ such that $v(t_n) = v_n$ where v_n is the observed state of the orbit at time t_n. With other words: There is a unique continuous T_p-periodic interpolating function of the data $(t_n, v_n), n = 1, 2, 3, ...$*

Proof. Let $V(\varphi)$ be the 1-periodic function given by the state v along γ. Let $\Phi : s \mapsto \varphi$ be the coordinate transformation from Assumption **A**. Set $v(s) := V(\Phi(s))$ and extend this function periodically.
This is true for all measure points ξ. Hence we get a continuous T_p-periodic function $t \mapsto v(\xi, t \bmod T_p)$. Since the reduced Poincaré map depends continuously on the the measure point ξ, we get a continuous function $v : [0, L) \times \mathbb{R} \to \mathbb{R}$, see Fig. 7 for $\xi = 0$ and $\xi = L/4$. Observe the scale on the speed axes and that time is running over two period intervals. Compare with Figure 4 for $\xi = 0$ and $\xi = L/4 = 3.25$.

Remark: Any $v(t_j) = v_j$ leads to some function value $v(s)$ for $s \in [0, T_p)$ with $s := s_j = t_j \bmod T_p$. To get a visualized "continuous" function v on $[0, T_p]$ we need a net $s_j, j = 1, 2, ..., k$ for not too large k which is approximately "dense" in $[0, T_p]$. The visualized denseness depends also on the thickness of the trajectories.

4 Computation of the macro period

Theorem 1. *Let us stop the sequence at a discrete time n, obtaining the angles $\varphi_0 = 0, \varphi_1, ..., \varphi_n$. Let φ_ℓ (φ_r) be the left (right) neighbor of $\varphi_0 = 0$ on S^1. Let $z_r \in \mathbb{N}$ be the number of rounds, the orbit has (just!) circled when reaching φ_r at (discrete) "time" r and let $z_\ell \in \mathbb{N}_0$ be the number of rounds, the orbit has (almost!) circled when reaching φ_ℓ at "time" ℓ. Then the following holds.*

$$\frac{t_\ell}{z_\ell} < T_p < \frac{t_r}{z_r}$$

Remark: It is known that for the rotation number

$$\frac{z_\ell}{\ell} < \varrho < \frac{z_r}{r}$$

holds. The bounds are Farey-neighbors, the next discrete time q when another orbit point is located in the interval $(\varphi_\ell, \varphi_r)$, is given by $q = \ell + r$. The MacKay algorithm ([Mac92]) for the computation of ϱ is based on this fact.

Proof. The claim follows from the "order-preserving" - assumption **A**.

5 Global flow

The local flow at some position is given by the number of cars per time unit which pass this position. Globally it is the average local flow which must be the same at any position of the circle. We take the observer point $\xi = 0$. Then obviously the local flow is the inverse of the actual wait time while the global flow f can be defined by $1/\tau$, where τ is the average wait time. For POMs the wait time is constant and equals the Nth part of the circulation time T. We get the simple formula $f = N/T$ where T is the orbital period (we have $T = N \cdot \tau$).
For quasi-POMs we can compute the average wait time by first computing the rotational number ϱ of the invariant curve and the macro-period T_p by MacKay-algorithm. Then we can set (see (12))

$$\tau = \varrho \cdot T_p.$$

Here we have observed an interesting point. If the center of the invariant curve is chosen in a wrong way, the resulting numbers ϱ and T_p were wrong, but $\tau = \varrho \cdot T_p$ was correct. On the other hand we could easily compute the time average of the wait time along a long orbit under the reduced Poincaré map.
The global flow is a very good characterizing quantity of the POMs and quasi-POMs, especially when one compares dynamics for different L, N and ε. For our solution diagrams we have observed the interesting fact that starting with the bottleneck-free case $\varepsilon = 0$ along the POM-branch the global flow decreases continuously. Moreover, a local increase of ε never leads to an increase of flow at a stable POM. Only unstable POMs may have this property.
For quasi-POMs it may be interesting to compare their flow with that of coexisting (mostly unstable) POMs. In some cases, we have observed a larger flow of quasi-POMs than that of coexisting POMs.

6 Numerical Results

In the sequel we refer to the quasi-POMs and their macroscopic visualizations and invariant curves presented in [GW10] for $N = 10, L = 13, a = 2, \tau = 1, v_{max} = 1$ and several values of $\varepsilon \in [0, 0.33]$. We will compute the rotation number ϱ and the macro time period T_p by the MacKay algorithm ([Mac92]) which is based on Lemma 1. For this purpose we have to assume that we have already found a quasi-POM by numerical simulation. Then we need a suitable headway-speed-plane for a certain car such that the projection of the corresponding invariant curve on this plane is star shaped with respect to a point M in its interior. If this is not possible, we can use a more general idea, see below.
The main aim is to compute the macroscopic speed function $v(\xi, t)$, where $0 \le \xi \le L$ and $0 \le t \le T_p$, by the projection method based on our Theorem 1. To this end we have to solve our $2N$-ODE system from $t = 0$ to $t = m \cdot T_p$ for a sufficiently large $m \in \mathbb{N}$ and to set

$$v(x_j(t) \bmod L, t \bmod T_p) = \dot{x}_j(t), j = 1, 2, ..., N.$$

The number m determines the numerical effort for the numerical simulation from $t = 0$ to $t = mT_p$. To obtain a "continuous" visualization result, i.e. a sufficiently dense net of points $(\xi, t \bmod T_p)$, m must be chosen large enough.

The choice of m depends on properties of ϱ (and on the graphical thickness of lines). The smaller ϱ and the more irrational ϱ is, the smaller m. The irrationality of ϱ depends on the continuous fraction expansion of ϱ.
We will also compute the time-angle function Φ and plot the angle φ as (discrete) function of time $t \in [0, T_p)$ to check whether assumption **A** holds. It holds, if we obtain a continuous, strictly monotone increasing function.

6.1 $\varepsilon = 0.3$

In the last sections we have already presented some figures for $\varepsilon = 0.3$. Here the projection of the corresponding invariant curve on the headway-speed plane of car No. 4 (counted from the measure point) is star shaped with respect to a point M in its interior, as can be seen from Figure 5.
The MacKay algorithm for 1000 iterations of the reduced Poincaré map yields the inclusions

$$0.06764 = \frac{60}{887} < \varrho < \frac{23}{340} = 0.06765 \tag{13}$$

and

$$32.73513 < T_p < 32.73674.$$

Hence, the average wait time $\tau = T_p \cdot \varrho$ fulfills (see (12))

$$2.21434 < \tau < 2.21454.$$

The fractions in (13) are so-called *convergents* of ϱ. With respect to the number $n = 1000$ of iterates of the reduced Poincaré map the inclusion in (13) is rather accurate. For $n = 5000$ iterations we get the inclusion

$$0.06764428 = \frac{143}{2114} < \varrho < \frac{226}{3341} = 0.06764442 \tag{14}$$

with more accurate $T_p = 32.7364$ and $\tau = 2.2144$.

Now we are going to explain our projection step for the computation of the macroscopic function $v(\xi, t)$. We have to choose two parameters, the number m for the simulation of the ODE-system for $t \in [0, m \cdot T_p]$ and the Matlab thickness d of the trajectory lines in the figures, see Figure 8 for different choices of m and d.

In Figure 9 we demonstrate how an inaccurate T_p can destroy the projection method. The result is obviously discontinuous.

6.2 $\varepsilon = 0.32$

In this case, the projection method is suffering under the special property of ϱ of being well approximable by the rational number $\frac{1}{13}$ with small denominator.
The MacKay algorithm for 500 iterations of the reduced Poincaré map yields the inclusions

$$0.07676768 = \frac{38}{495} < \varrho < \frac{1}{13} = 0.07692308 \tag{15}$$

and

$$29.30249756 < T_p < 29.36220498.$$

Hence, the average wait time $\tau = T_p \cdot \varrho$ fulfills (see (12))

$$2.24948466 < \tau < 2.25863115.$$

For 1000 iterates we get the much better inclusion

$$0.07680492 = \frac{50}{651} < \varrho < \frac{51}{664} = 0.07680723 \tag{16}$$

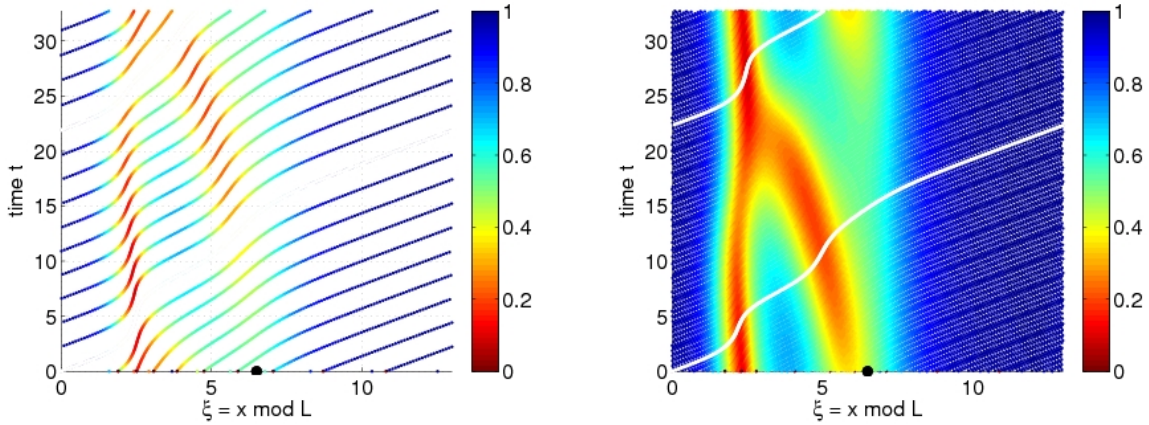

(a) $m = 1, d = 5$

(b) $m = 10, d = 5$

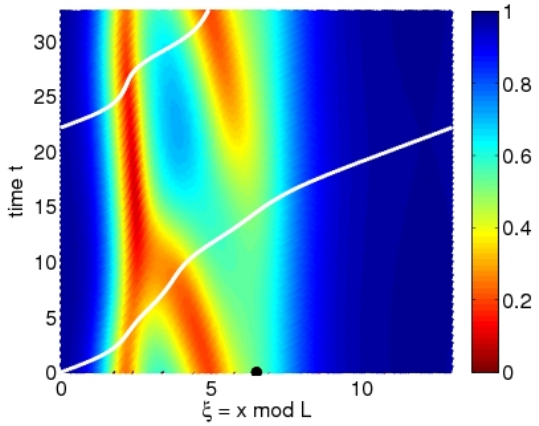

(c) $m = 50, d = 5$

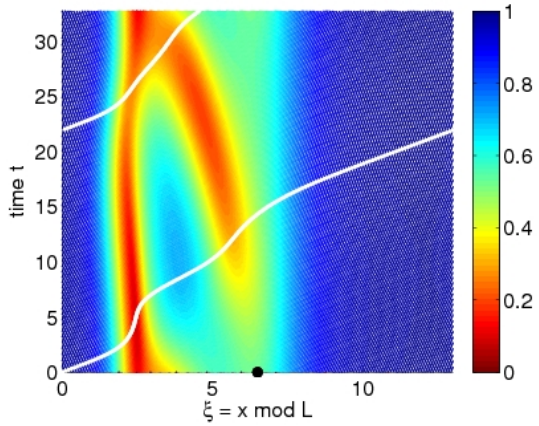

(d) $m = 50, d = 1$

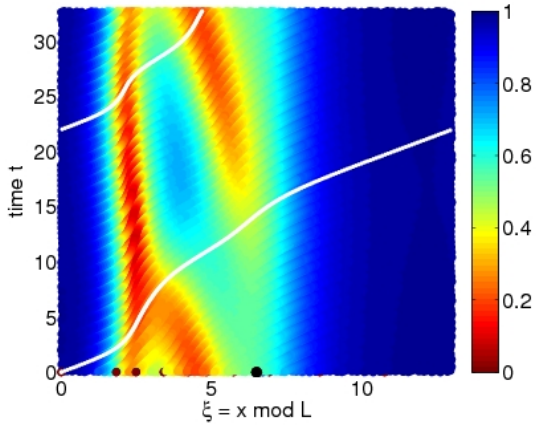

(e) $m = 10, d = 40$

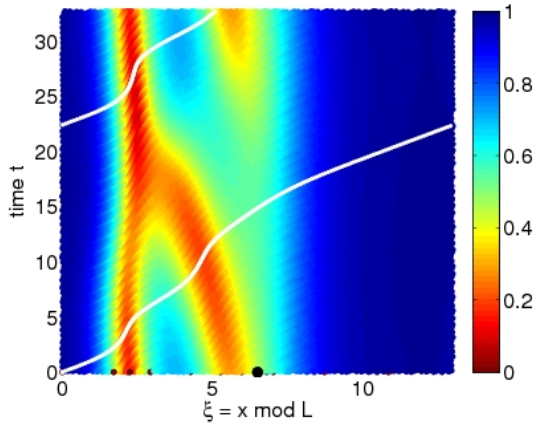

(f) $m = 10, d = 20$

Figure 8: $N = 10, L = 13, \varepsilon = 0.3, T_p = 32.74$: Macroscopic visualization of the speed function v for different values of m and d.

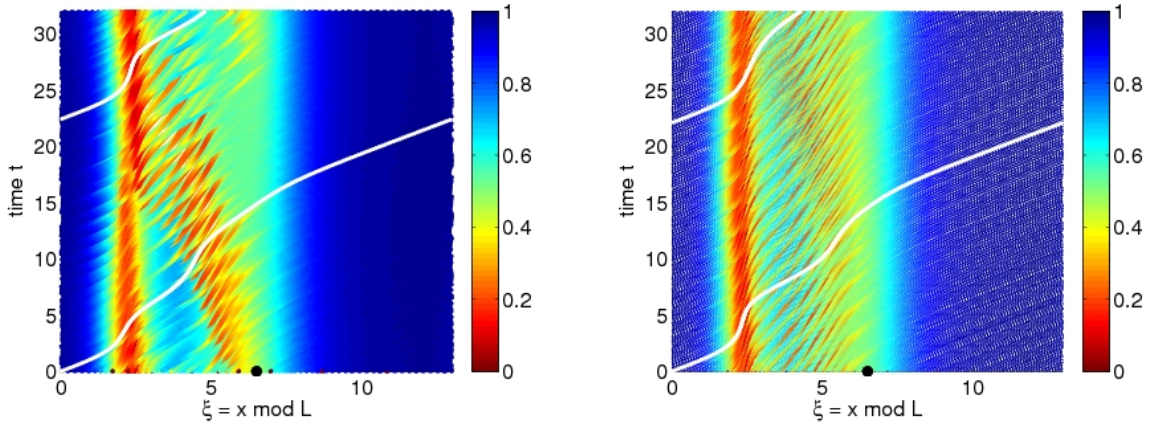

(a) $m = 20, d = 10$ (b) $m = 50, d = 1$

Figure 9: $N = 10, L = 13, \varepsilon = 0.3$: macroscopic visualization of a discontinuous speed function for an inaccurate $T_p = 32$ instead of $T_p = 32.74$.

and

$$29.34697180 < T_p < 29.347866220498.$$

Hence, the average wait time $\tau = T_p \cdot \varrho$ fulfills (see (12))

$$2.25399169 < \tau < 2.25412786.$$

The consequences of the fact that $\frac{1}{13}$ is a very good upper bound of ϱ (every fraction which is a better upper bound has a denominator larger than 600), can be seen in Figure 10 which shows the result of the projection method for different values of m. Here we always used the relatively small Matlab line thickness $d = 5$. Only for $m = 50$ the projection method yields a macroscopic acceptable picture.

6.3 $0.0 \leq \varepsilon \leq 0.25$

In this section we want to compute the macro period T_p for all cases reported in [GW10]. The main difficulty is to find suitable polar coordinates by projections of the invariant curve on an appropriate plane such that the encircled region is star like to a center. To check the assumption **A** we will compute some time-angle functions (which depend on the chosen polar coordinates), the projected invariant curve (which depends on the type of projection) and most important the macro period T_p with lower and upper bounds. As¡already mentioned, the accuracy depends on the number of iterations performed for the reduced Poincaré map and on the irrationality of the rotation number ϱ.
Observe that for the values $\varepsilon = 0.25$ and $\varepsilon = 0.27$ there coexist two different quasi-POMs.

1. $\boldsymbol{\varepsilon = 0.0}$.

   The projection of the IC on the headway-speed plane of car No. 4 is starlike wrt $M = [0.75, 0.35]$. Assumption A seems to be satisfied according to Fig. 11.

   After 1000 iterations of the reduced Poincaré map we get the following inclusions:

   $$189.79299140 < T_p < 189.90078628$$

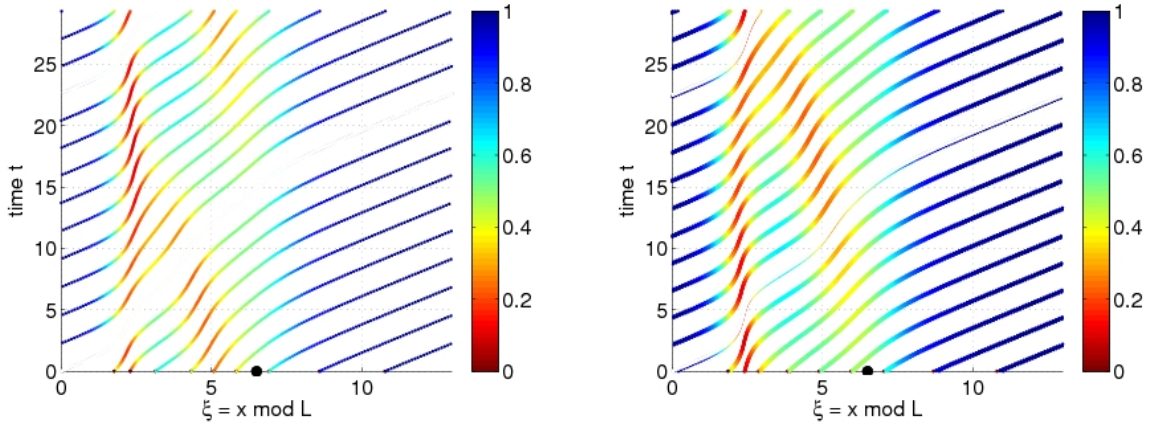

(a) $m = 1$ (b) $m = 5$

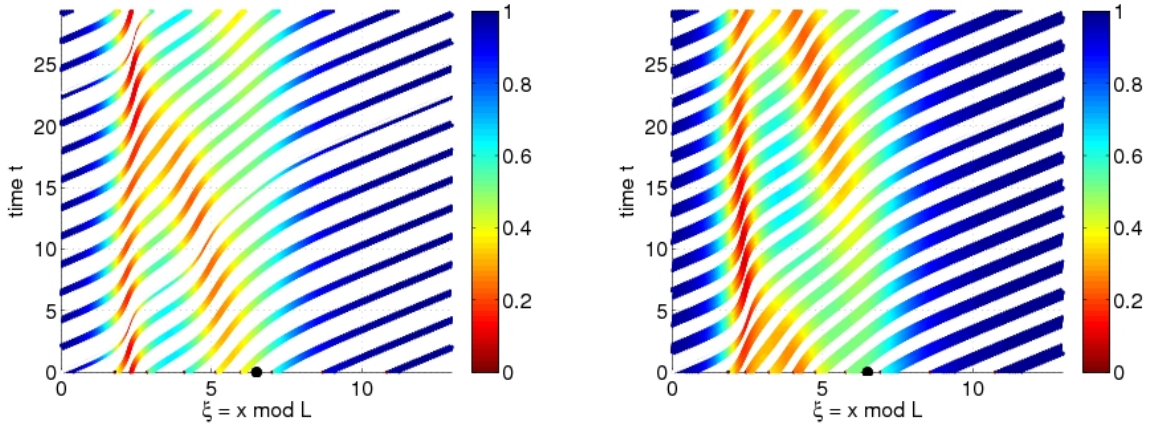

(c) $m = 10$ (d) $m = 20$

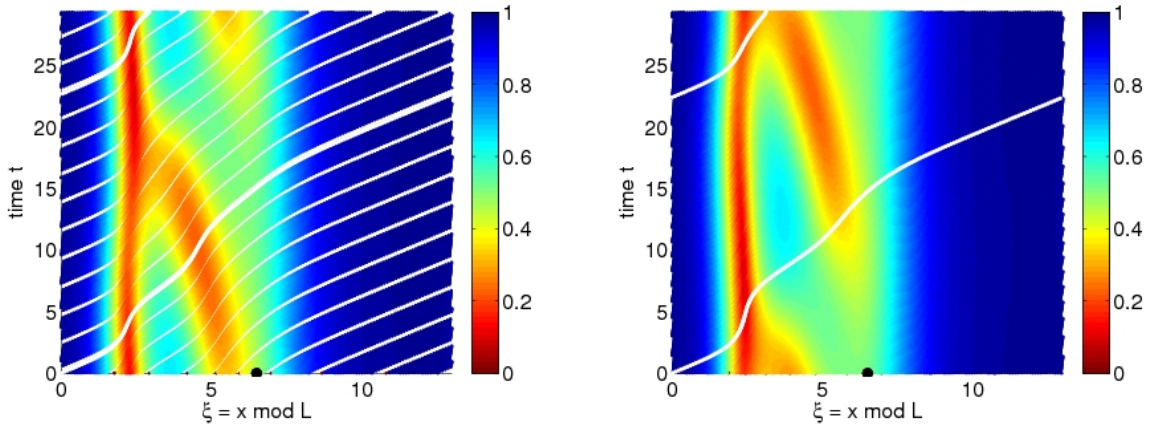

(e) $m = 40$ (f) $m = 50$

Figure 10: $N = 10, L = 13, \varepsilon = 0.32, T_p = 29.347, d = 5$: Macroscopic visualization of the speed function v for different values of m.

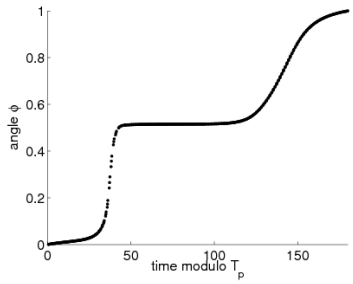

Figure 11: time-angle function Φ for $\varepsilon = 0.0$ and car No. 4

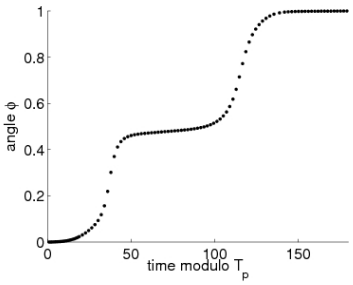

Figure 12: time-angle function Φ for $\varepsilon = 0.1$ and car No.4

$$\frac{2}{193} < \varrho < \frac{9}{868}, \quad 0.01036269 < \varrho < 0.01036866, \quad 1.96676675 < \tau < 1.96901737.$$

After 5000 iterations we get the more accurate estimation $189.81994188 < T_p < 189.82210118$.

2. $\boldsymbol{\varepsilon = 0.1}$. The projection of the IC on the headway-speed plane of car No. 4 is starlike again wrt $M = [0.75, 0.35]$. Assumption **A** seems to be satisfied according to Fig. 12.

   After 1000 iterations of the reduced Poincaré map we get the following inclusions:

$$180.12339642 < T_p < 180.15322845$$

$$\frac{7}{634} < \varrho < \frac{9}{815}, \quad 0.01104101 < \varrho < 0.01104294, \quad 1.98874412 < \tau < 1.98942215.$$

   The rotation number is sufficiently irrational for our computations.

   After 5000 iterations we get the better inclusion $180.12815764 < T_p < 180.12955231$.

3. $\boldsymbol{\varepsilon = 0.2}$. The projection of the IC on the headway-speed plane of car No. 3 (not for car No.4!) is starlike wrt $M = [0.75, 0.35]$. Assumption A seems to be satisfied according to Fig. 13.

   After 1000 iterations of the reduced Poincaré map we get the following inclusions:

$$175.49563670 < T_p < 175.52290665$$

$$\frac{10}{873} < \varrho < \frac{7}{611}, \quad 0.01145475 < \varrho < 0.01145663, \quad 2.01025881 < \tau < 2.01090124.$$

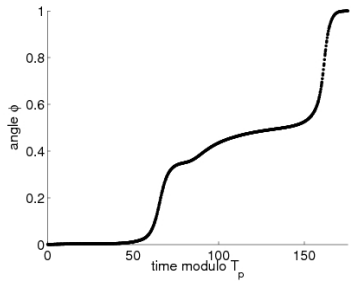

Figure 13: time-angle function Φ for $\varepsilon = 0.2$ and car No.3

The rotation number is sufficiently irrational for our computations.

After 5000 iterations we get $175.50688700 < T_p < 175.50894549$.

4. $\boldsymbol{\varepsilon = 0.24}$.

   There are no projections of the IC on a headway-speed plane of single cars which are star like wrt to a point, see Fig. 14.

   To compute the macro period T_p we need another method to find suitable polar coordinates. We succeeded by using the average of three-car datas headway and speed with center $M = (0.75, 0.35)$. The assumption **A** is satisfied, see Fig. 15.

   Using 5000 iterations we get

   $$162.99452500 < T_p < 162.99643851$$

   and

   $$\frac{47}{3822} < \varrho < \frac{22}{1789}, \quad 0.01229723 < \varrho < 0.01229737, \quad 2.00438061 < \tau < 2.00442798.$$

5. $\boldsymbol{\varepsilon = 0.25}$.

   Using 5000 iterations we get

   $$94.94346935 < T_p < 94.94382682$$

   and

   $$\frac{53}{2473} < \varrho < \frac{103}{4806}, \quad 0.02143146 < \varrho < 0.02143154, \quad 2.03477714 < \tau < 2.03479279.$$

   Observe the dramatic change in comparison with $\varepsilon = 0.24$.

6. $\boldsymbol{\varepsilon = 0.27}$.

   Also here our average projection works with the same center though also the single car projection would have worked too.

   Using 5000 iterations we get

   $$39.71481676 < T_p < 39.71495430$$

   and

   $$\frac{263}{4841} < \varrho < \frac{59}{1086}, \quad 0.05432762 < \varrho < 0.05432781, \quad 2.15761140 < \tau < 2.15762643.$$

   There is a second coexisting quasi-POM, see [GW10].

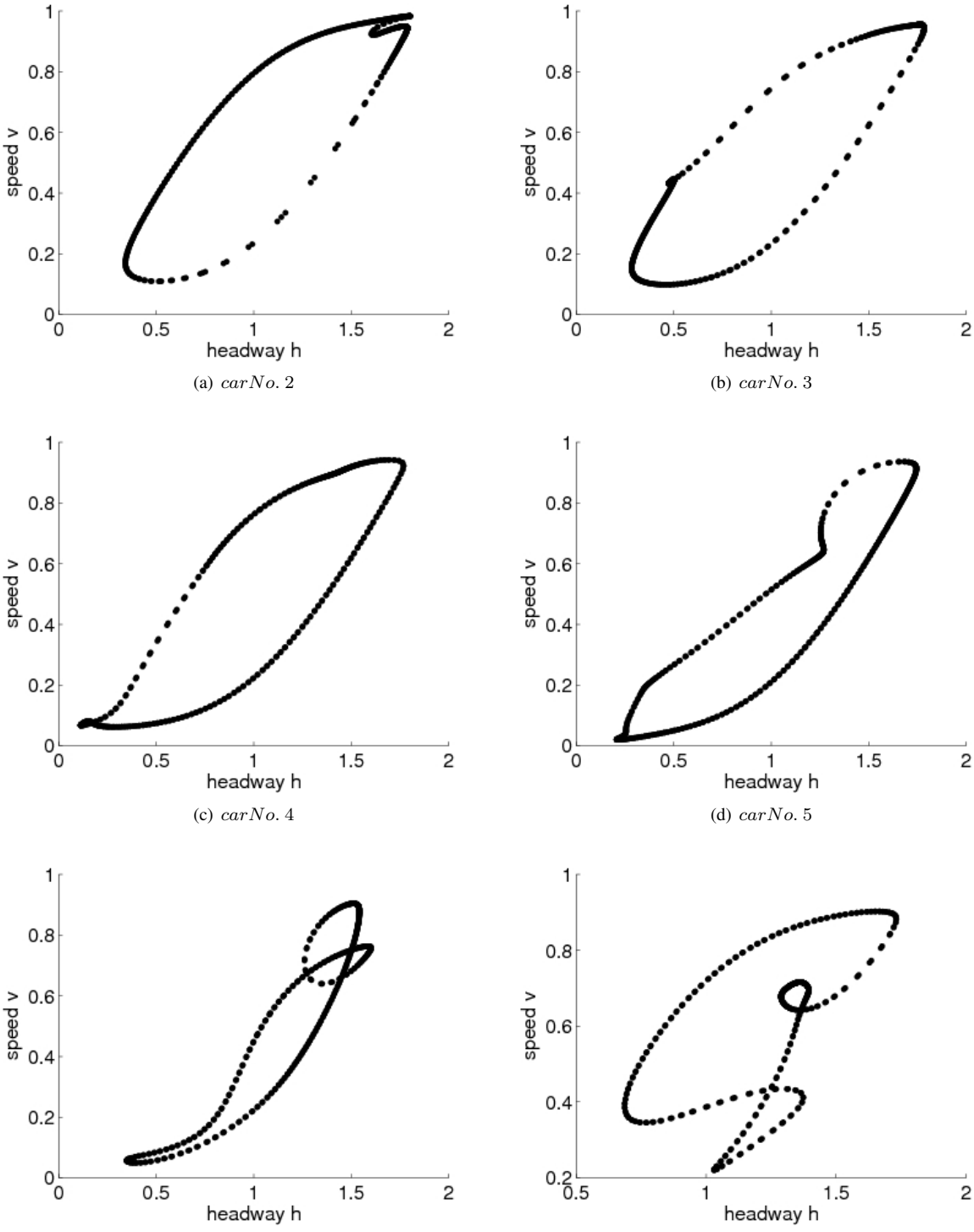

(a) $carNo.\ 2$ (b) $carNo.\ 3$

(c) $carNo.\ 4$ (d) $carNo.\ 5$

(e) $carNo.\ 6$ (f) $carNo.\ 7$

Figure 14: $N = 10, L = 13, \varepsilon = 0.24$: Different projections of the IC on headway-speed planes of different cars.

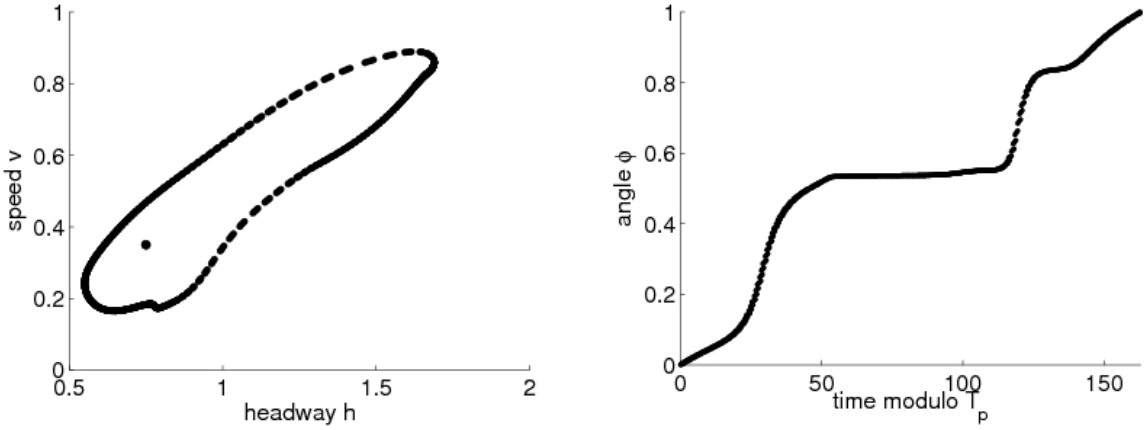

(a) Invariant curve (b) time-angle function

Figure 15: $N = 10, L = 13, \varepsilon = 0.24$: Average projection car No. 3, 4, 5

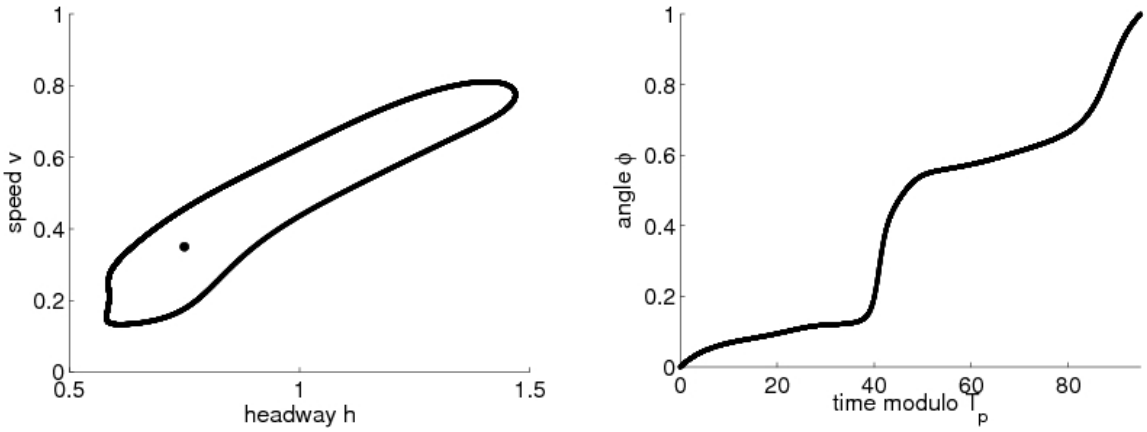

(a) Invariant curve (b) time-angle function

Figure 16: $N = 10, L = 13, \varepsilon = 0.25$: Average projection car No. 3, 4, 5

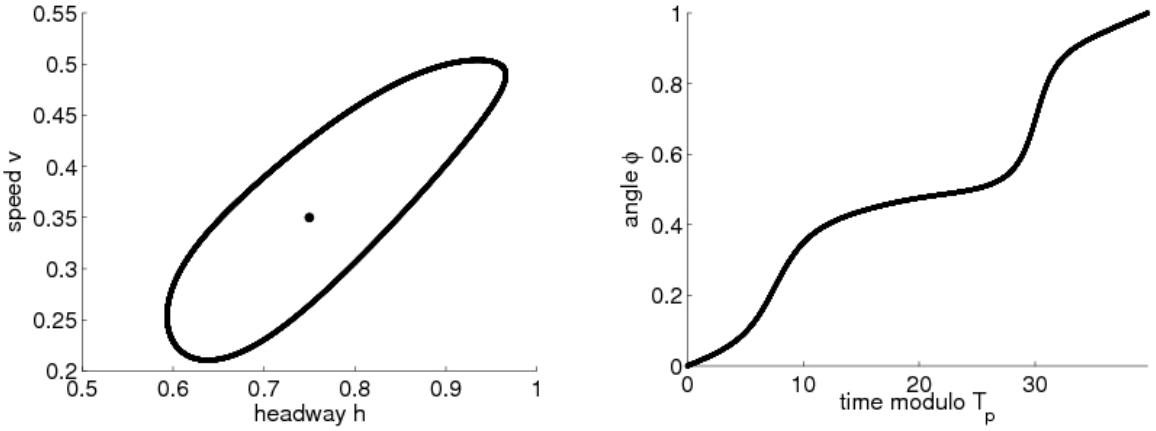

(a) Invariant curve

(b) time-angle function

Figure 17: $N = 10, L = 13, \varepsilon = 0.27$: Average projection car No. 3, 4, 5

After 2000 iteration steps we get

$$43.30870976 < T_p < 43.30939547$$

and

$$\frac{65}{1318} < \varrho < \frac{47}{953}, \quad 0.04931715 < \varrho < 0.04931794, \quad 2.13586201 < \tau < 2.13593031.$$

7. $\boldsymbol{\varepsilon = 0.25}$. This quasi-POM which coexists with that described above for the same value of $\varepsilon = 0.25$. It can be obtained by a kind of path following. The polar coordinates can be easily chosen by projection on the headway-speed plane of a single car (No.5), the macro period is much less, the average wait time is larger than that of the coexisting quasi-POM.

   After 2000 iterations we get

$$49.59085527 < T_p < 49.59921633,$$

$$\frac{15}{353} < \varrho < \frac{17}{400}, \quad 0.04249292 < \varrho < 0.04250000, 2.10726014 < \tau < 2.10796669.$$

7 Additional remarks

1. The theory does not depend on the assumption of identical drivers. It is also valid for quasi-rotations, see Section **??**. We expect similar periods, but different patterns, since the macroscopic functions will be different for different cars. The simulations will be much more expensive than for the case of identical drivers.

2. In this paper, our projection method is only used for macroscopic visualizations. But of course, it could also be used for an analytical expression for $v(\xi, t)$ by some approximation method based on interpolating data. This expression could be used to compute numerically an arbitrary run of a car by solving the scalar (!) ODE

$$\dot{\xi} = v(\xi, t), \quad \xi(0) = \xi_0.$$

3. It would be tempting to try to compute the observer function $v(\xi, t)$ directly as a T_p periodic function comparable to the computation of periodic solutions of ODEs. But this is impossible since these functions (as the invariant curves themselves) do not depend smoothly on parameters. The Implicit Function Theorem does not hold. Hence the computation of such observer functions is somewhere ill posed.

References

[AGMP91] D. G. Aronson, M. Golubitsky, and J. Mallet-Paret. Ponies on a merry-go-round in large arrays of josephson junctions. *Nonlinearity*, 4:903–910, 1991.

[BHN+95] M. Bando, K. Hasebe, A. Nakayama, A. Shibata, and Y. Sugiyama. Dynamical model of traffic congestion and numerical simulation. *Phys. Rev. E*, 51:1035ff, 1995.

[BJ08] L. Buřič and V. Janovský. On pattern formation in a class of traffic models. *Physica D 237*, 2008.

[dMvS91] W. de Melo and S. van Strien. *One-dimensional Dynamics*. Springer, 1991.

[GH83] J. Guckenheimer and P. Holmes. *Nonlinear Oscillations, Dynamical Systems and Bifurcations of Vector Fields.*, volume 42 of *Applied Mathematical Sciences*. Springer, 1983.

[GSW04] I. Gasser, G. Sirito, and B. Werner. Bifurcation analysis of a class of 'car following' traffic models. *Physica D*, 197/3-4:222–241, 2004.

[GW10] I. Gasser and B. Werner. Dynamical phenomena induced by bottleneck. *Phil. Trans. R. Soc. A 368, 4543-4562*, 2010.

[Mac92] R.S. MacKay. Rotation interval from a time series. *J. Phys.*, A 20:587–592, 1992.

[SGW09] T. Seidel, I. Gasser, and B. Werner. Microscopic car-following models revisited: from road works to fundamental diagrams. *SIAM J. Appl. Dyn. Sys. 8, 1305-1323*, 8 (3):1305–1323, 2009.

[Wer11] B. Werner. An asymptotic numerical analysis of hopf periodic traveling waves for a microscopic traffic problems. *Hamburger Beiträge zur Angewandten Mathematik*, 2011.